

Quark substructure approach to ^4He charge distribution

L. Wilets and M. A. Alberg*

Department of Physics, Box 351560, University of Washington, Seattle, Washington 98195-1560

S. Pepin and Fl. Stancu

Université de Liège, Institut de Physique B.5, Sart Tilman, B-4000 Liège 1, Belgium

J. Carlson

Theoretical Division, Los Alamos National Laboratory, Los Alamos, New Mexico 87545

W. Koepf

Department of Physics, The Ohio State University, Columbus Ohio 43210

(Received 19 December 1996)

We present a study of the ^4He charge distribution based on realistic nucleonic wave functions and incorporation of quark substructure. Any central depression of the proton point density seen in modern four-body calculations is too small by itself to lead to a correct description of the charge distribution of ^4He if folded with a fixed proton size parameter, as is usually done. We utilize six-quark structures calculated in the chromodis-electric model for N - N interactions to find a “swelling” of the proton size as the internucleon distance decreases. This swelling is a result of the short-range dynamics in the N - N system. Using the independent pair approximation, the corresponding charge distribution of the proton is folded with the two-nucleon distribution generated from Green’s function Monte Carlo calculations of the ^4He nucleonic wave function. We obtain a reasonably good fit to the experimental charge distribution of ^4He . Meson-exchange currents have not been included. [S0556-2813(97)04207-6]

PACS number(s): 21.45.+v, 13.75.Cs, 21.30.Fe, 24.85.+p

I. INTRODUCTION

The charge distribution of nuclei has been the subject of experimental studies for more than forty years. Electron scattering and muonic atoms now provide detailed descriptions of the full range of stable, and many unstable nuclides. Unique among the nuclides are the isotopes ^3He and ^4He because they exhibit a central density about twice that of any other nuclei. There is a long-standing apparent discrepancy between the experimentally extracted charge distributions and detailed theoretical structure calculations which include only nucleon degrees of freedom.

McCarthy, Sick, and Whitney [1,2] performed electron scattering experiments on these isotopes up to momentum transfers of 4.5 fm^{-1} yielding a spatial resolution of 0.3 fm . They extracted a “model-independent” charge distribution, which means that their analysis of the data is not based upon any assumed functional form for the charge distributions. Their results are shown in Fig. 1. Taken alone, they do not appear to be extraordinary. However, using the experimentally measured proton form factor, which has a fixed rms radius of about 0.83 fm , they unfolded the proton structure from the charge distributions to obtain proton point distributions. For both isotopes they found a significant central depression of about 30% extending to about 0.8 fm . Sick [2] also obtained results where relativistic and meson effects were considered. These are shown for ^4He in Fig. 2. One

note of caution here is that it is not possible to subtract these effects from the experimental data in a completely model-independent way.

One might assume that such a central depression is to be expected because of the short-range repulsion of the nucleon-nucleon interaction. This is not borne out by numerous detailed theoretical calculations (see, for example, Ref. [3]) none of which finds a *significant* central depression, certainly not of the above magnitude. Relatively smaller central depressions are found in Green’s function Monte Carlo (GFMC) calculations of ^4He for realistic models of the two- and three-nucleon interaction [4,5].

The status of theoretical structure calculations through mass number 4 is very satisfactory at present. Given any assumed interaction, the few body problem can be solved to within tenths of an MeV in energy and the wave function can be calculated to a precision better than that required for the present discussion.

In using a nucleonic wave function to construct a charge distribution, one must use (1) an assumed proton charge density and (2) consider the possibility of meson exchange contributions. While the meson exchange contributions in the transverse channel are well constrained (at least at moderate momentum transfer) by current conservation, no such constraint is available in the longitudinal channel. Indeed, meson exchange contributions are of relativistic order and hence one must be careful when interpreting them with nonrelativistic wave functions [4–6].

Here we discuss the role of the proton charge density and present a possible explanation of the electric form factor of ^4He , which is consistent with theoretical few-body calcula-

*Permanent address: Department of Physics, Seattle University, Seattle WA 98122.

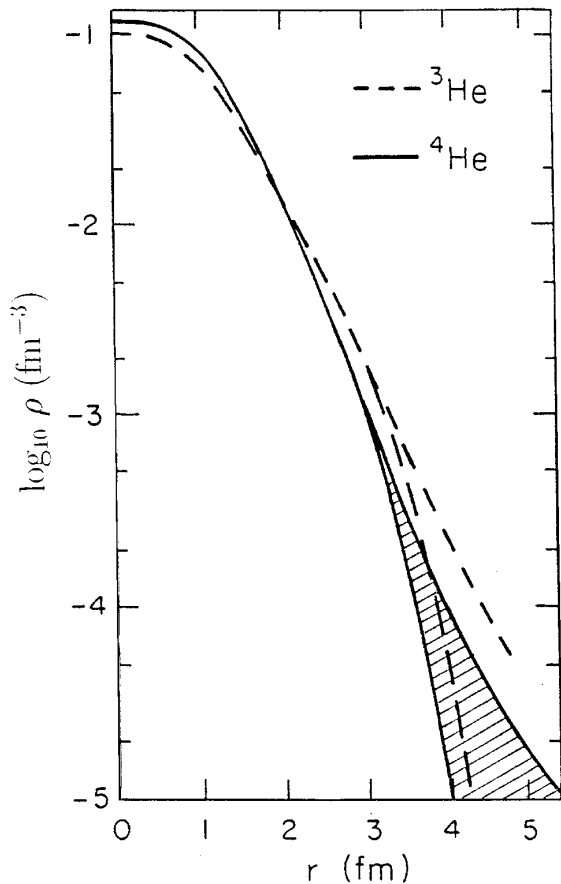


FIG. 1. Model-independent charge distributions for ${}^3\text{He}$ and ${}^4\text{He}$ extracted from experiment. Reproduced from McCarthy *et al.* [1], who state that “the extreme limits of $\rho(r)$ cover the statistical, systematic as well as the completeness error of the data.”

tions and is based on the quark structure of nucleons. The big depression found by McCarthy *et al.* in the proton-point distribution was obtained by unfolding the *free* proton form factor from the experimental charge distribution. Here we will assume a variation of the proton charge form factor (size) as a function of internucleon separation. This is not depicted as an average “swelling” of the nucleon, but as a result of short-range dynamics in the nucleon-nucleon system, as discussed in the next section. We relate the variation of the proton size to the quarks dynamics, here described by the chromodielectric soliton model (CDM). We will show that the combination of the proton point density obtained by realistic four-body calculations with a variable proton form factor reproduces qualitatively well the ${}^4\text{He}$ charge distribution. Our work is similar in spirit, but different in details, from that of Kisslinger *et al.* [7], where the role of multi-quark cluster in describing the ${}^3\text{He}$ charge distribution has been pointed out. The common idea is that the form factors in quark or soliton based models would describe the short-range two-body structure of the nucleons in a more direct way than is available through meson-exchange current models.

In Sec. II, we explain how we derived a variable proton size from six-quark calculations and show how to calculate the ${}^4\text{He}$ charge distribution in the independent pair approximation. In Sec. III, we first briefly describe the calculations

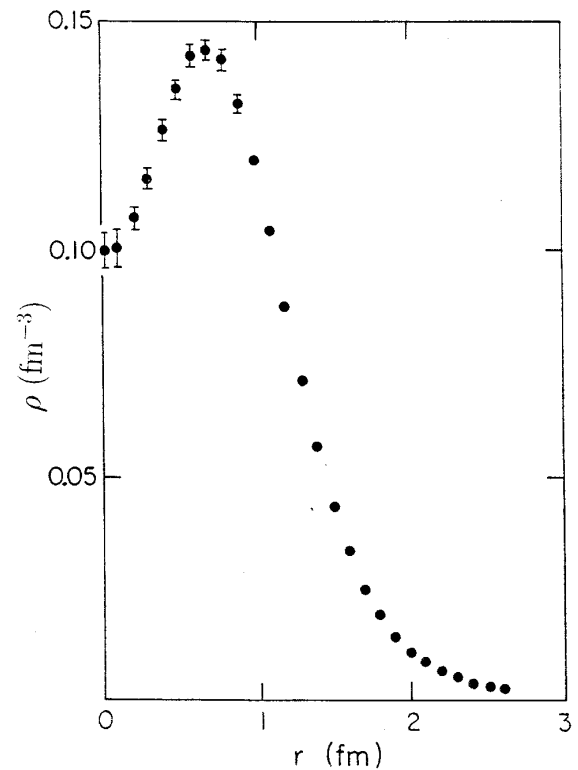


FIG. 2. Point-proton density distribution for ${}^4\text{He}$ obtained by unfolding the free proton form factor, allowing for meson exchange corrections and relativistic effects. Reproduced from Sick [2].

of the ${}^4\text{He}$ wave function (from which the point-density is deduced) by using Green’s function Monte Carlo method. Then we present our results for the ${}^4\text{He}$ charge distribution. Finally, Sec. IV sketches some conclusions.

II. QUARK SUBSTRUCTURE OF NUCLEI AND NUCLEONS

A large number of papers have investigated the effects of the quark substructure on nuclear phenomena. Clustering of nucleons into six-quark structure has been claimed to account for the EMC effect [8] (this claim has, however, been put into question by a recent work of Koepf and Wilets [10], see the discussion below). Kisslinger *et al.* [7] used a hybrid quark-hadron model to calculate explicitly the contribution of six-quark and nine-quark clusters to the electric and magnetic form factor of $A=3$ nuclei.

In a series of papers, Koepf, Pepin, Stancu, and Wilets [9–11] have studied the six-quark substructure of the two-nucleon problem in the framework of the chromodielectric soliton model [12]. The CDM is a relativistic quark bag model. Its Lagrangian is the same as the fundamental QCD Lagrangian except for the gauge field part; it is supplemented by a scalar field, which parametrizes the bulk of the nonperturbative effects due to the nonlinearity of QCD. This scalar field generates a chromodielectric function, which leads to color confinement.

In the six-quark problem, we obtained the scalar field in a constrained mean-field calculation. Instead of specifying the constraint function, we solved the equations for the scalar and the quark fields simultaneously and self-consistently for

each value of a collective deformation parameter α (see Eqs. (13) and (14) of Ref. [9]). Quark wave functions were obtained as a function of this parameter, which describes the geometrical shape of the six-quark bag. Large value of α correspond to two well-separated nucleons, $\alpha=0$ to a spherical six-quark bag and negative α to oblate deformations of the bag. In the calculation of the six-quark wave function, by using molecular orbitals, we introduced configuration mixing with higher quark states. In a first step [9], a local nucleon-nucleon potential was calculated in the Born-Oppenheimer approximation as a function of α . In a second step [11], the generator coordinate method was used to treat the N - N interaction dynamically. An approximate Hill-Wheeler differential equation for the N - N wave function was derived. In order to write a Schrödinger-like equation for the N - N wave function, the deformation parameter α was related to an effective internucleon separation r_{NN} by the so-called Fujiwara transformation. This internucleon separation will be used here in the calculations of the quark substructure of the nuclei.

In [10], the momentum distribution in the N - N system was derived from these six-quark calculations. Contrary to previous expectation, the united six-quark cluster does not exhibit a significant decrease in the quark momentum in spite of an increase in the volume available to the individual quarks. This is due to configuration mixing of higher quark states. Such a momentum decrease had been proffered as an explanation of the EMC effect [13]. Nevertheless, the united cluster does have approximately twice the confinement volume of each three-quark cluster, and the quarks extend to a volume nearly three times that of the three-quark clusters, again enhanced by configuration mixing of excited states.

From the six-quark wave functions obtained as described above, we calculated $\langle r^2 \rangle = \int \rho_q r^2 d^3r$ as a function of α or equivalently of r_{NN} . (Here ρ_q is the six-quark density normalized to unity.) This is used to define an effective nucleon size as

$$r_p = \sqrt{\langle r^2 \rangle - r_{NN}^2/4}. \quad (1)$$

Figure 3 exhibits r_p as a function of r_{NN} . For separated solitons, the r_{NN} is just the separation of the soliton centers and $r_p = 0.83$ fm as indicated by the horizontal line labeled ‘‘free proton’’ in Fig. 3. Since large deformations (near separation) are difficult to calculate, we terminate the figure at 2.0 fm. Shown also in the figure is a Gaussian approximation (dashed line) fitted to the CDM result at $r_{NN}=0$, $r_{NN}=1$ fm, and in the asymptotic region according to

$$r_p(r') = r_0 [1 + A e^{-r'^2/s^2}], \quad (2)$$

with the free proton value $r_0 = 0.83$ fm, $A = 0.45$, and $s = 1.92$ fm.

We assume a Gaussian form for the variable proton charge density. The width b of this Gaussian is directly related to the effective nucleon size (2) by

$$b(r') = \sqrt{2/3} r_p(r'). \quad (3)$$

Then the charge distribution due to two nucleons is defined as

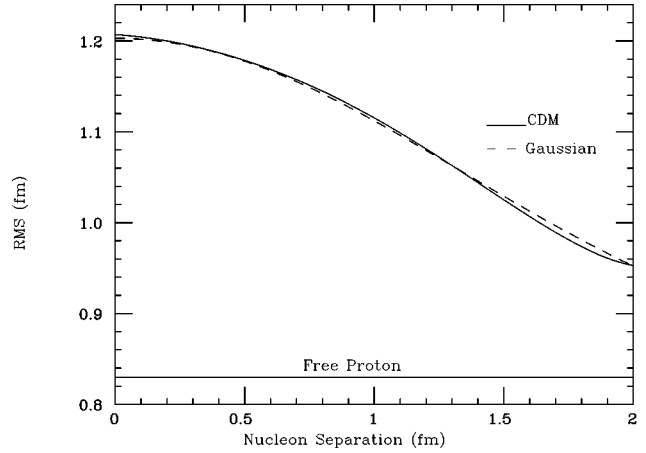


FIG. 3. Proton rms charge radius r_p of Eq. (1) as a function of internucleon separation. The line labeled CDM is the calculated chromodielectric model result. The dashed line is a Gaussian approximation, normalized to the free value, with a size parameter given by Eq. (3)

$$\begin{aligned} \rho_{\text{pair}}(\mathbf{r}_i, \mathbf{r}_j; \mathbf{r}) = & \{ \delta_{ip} \exp[-|\mathbf{r} - \mathbf{r}_i|^2/b^2(r_{ij})] \\ & + \delta_{jp} \exp[-|\mathbf{r} - \mathbf{r}_j|^2/b^2(r_{ij})] \} / \pi^{3/2} b^3(r_{ij}), \end{aligned} \quad (4)$$

where r_{ij} is the distance between the nucleons located at \mathbf{r}_i and \mathbf{r}_j and \mathbf{r} is the observation point. In the calculations of the six-quark wave functions, we did not distinguish the proton from the neutron. This is why we introduced Kronecker symbols δ_{ip} (where ‘‘p’’ stands for ‘‘proton’’) which pick out protons among the nucleons i and j .

In this study we use the independent pair approximation (IPA), which allows to reduce a four-body problem to a two-body one. Then, from Eq. (4), we can calculate the charge distribution as

$$\rho_{\text{ch}}(r) = \frac{1}{3} \sum_{i < j} \int d^3r_i \int d^3r_j f_2(\mathbf{r}_i, \mathbf{r}_j) \rho_{\text{pair}}(\mathbf{r}_i, \mathbf{r}_j; \mathbf{r}). \quad (5)$$

There are six pairs (i, j) and each proton appears three times, hence the factor 1/3. The two-body correlation function $f_2(\mathbf{r}_i, \mathbf{r}_j)$ is generated from the four-body nuclear wave function described in the next section by

$$f_2(\mathbf{r}_1, \mathbf{r}_2) = \int |\psi(\mathbf{r}_1, \mathbf{r}_2, \mathbf{r}_3, \mathbf{r}_4)|^2 d^3r_3 d^3r_4, \quad (6)$$

with the constraint $\mathbf{r}_1 + \mathbf{r}_2 + \mathbf{r}_3 + \mathbf{r}_4 = \mathbf{0}$.

III. ${}^4\text{He}$ CHARGE DISTRIBUTION: RESULTS

The two-body correlation function (6) requires the knowledge of the ${}^4\text{He}$ wave function $\psi(\mathbf{r}_1, \mathbf{r}_2, \mathbf{r}_3, \mathbf{r}_4)$, which has been obtained by solving the nonrelativistic Schrödinger equation

$$\left[\sum_i -\frac{\hbar^2}{2m} \nabla_i^2 + \sum_{i < j} V_{ij} + \sum_{i < j < k} V_{ijk} \right] \psi = E \psi, \quad (7)$$

where V_{ij} and V_{ijk} are the v_{18} Argonne nucleon-nucleon interaction and the Urbana 9 three-nucleon interaction, respectively. The general form of the two-body part is

$$V = \sum_{k=1}^{14} \sum_{i<j} V^k(r_{ij}) O_{ij}^k, \quad (8)$$

where the operators O_{ij}^k are

$$O_{ij}^k = 1, \vec{\sigma}_i \cdot \vec{\sigma}_j, S_{ij}, \vec{L} \cdot \vec{S}, L^2, L^2 \vec{\sigma}_i \cdot \vec{\sigma}_j, (\vec{L} \cdot \vec{S})^2, \quad (9)$$

with

$$S_{ij} = 3(\vec{\sigma}_i \cdot \vec{r}_{ij})(\vec{\sigma}_j \cdot \vec{r}_{ij}) - \vec{\sigma}_i \cdot \vec{\sigma}_j \quad (10)$$

the usual tensor operator, \vec{L} the relative orbital angular momentum, and \vec{S} the total spin of the pair. The O_{ij}^k operators above are either multiplied by the unit 2×2 matrix or by the isospin operator $\vec{\tau}_i \cdot \vec{\tau}_j$, which explains the 14 terms in Eq. (8).

The radial components $V^k(r_{ij})$ consist of a one-pion exchange interaction at long distances, an intermediate range attraction, and a short-range phenomenological repulsion with shapes as described in Ref. [14]. Their parameters are fitted to the deuteron and to the two-body scattering data. The three-nucleon interaction V_{ijk} consists of a long-range two-pion exchange piece and a short-range repulsive term. The parameters are determined by fitting the binding energy of $A=3$ nuclei.

The Schrödinger equation (7) has been solved by using the Green's function Monte Carlo (GFMC) method, which has proven to be very valuable in studying light nuclei, and produced more accurate results than the so-called variational Monte Carlo (VMC) method. A typical difference, important for the present study, is that within 0.5 fm of the center-of-mass the GFMC point density has a slight depression which does not appear in VMC results. Details about the GFMC method are reviewed in Ref. [5]. The combination of the potentials V_{ij} and V_{ijk} introduced above gives the correct binding energy and approximately the correct rms radius for ${}^4\text{He}$. Previous calculations of other properties of ${}^4\text{He}$ have been done with an older nucleon-nucleon interaction v_{14} [15].

We have calculated the charge distribution for ${}^4\text{He}$ in the spirit of the independent pair approximation using Eq. (4). The proton size parameter $b(\mathbf{r}_1 - \mathbf{r}_2)$ given by Eq. (3) was taken from the Gaussian fit to the calculations of Pepin *et al.* [11] presented in Fig. 3. The resulting distribution is shown in Fig. 4 (solid line). The improvement over the free proton case, i.e., a Gaussian with a constant $b = \sqrt{2/3}$ 0.83 fm (dotted line) is impressive and leads to fairly good agreement with the data. In the same figure we also indicate the point density (dashed line)

$$\rho(\mathbf{r}) = 2 \int |\psi(\mathbf{r}_1, \mathbf{r}_2, \mathbf{r}_3, \mathbf{r}_4)|^2 \delta(\mathbf{r} - \mathbf{r}_1) d^3r_1 d^3r_2 d^3r_3 d^3r_4, \quad (11)$$

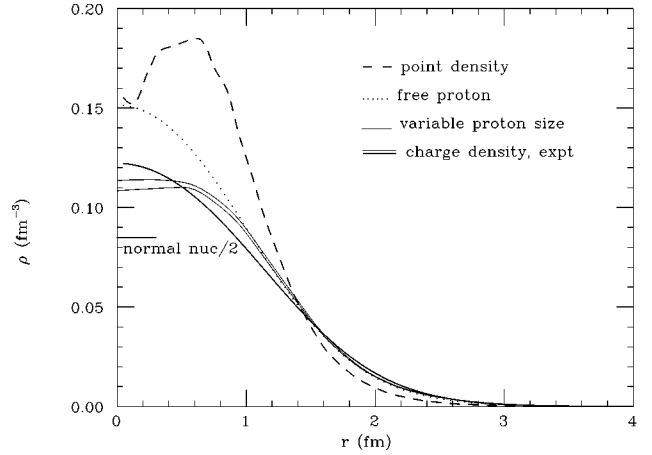


FIG. 4. ${}^4\text{He}$ density distributions: The dashed line is the point density from a parametrized Green's function Monte Carlo calculation. The curve labeled "free proton" is the charge distribution obtained from a Gaussian proton charge distribution with a fixed size parameter (as is usually done). The curve labeled "variable proton size" uses the Gaussian fit of Fig. 3. We also indicate half the normal nuclear density $0.17/2 \text{ fm}^{-3}$.

where ψ is the ${}^4\text{He}$ wave function described above. Note that the right-hand side of Eq. (11) can also be obtained from Eq. (5) where ρ_{pair} of Eq. (4) would contain δ functions instead of Gaussians. Even though this density shows a central depression, we have shown that it is not sufficient by itself to reproduce the data, when combined with the free proton form factor.

IV. CONCLUSIONS

We succeeded in reproducing fairly well the ${}^4\text{He}$ charge distribution by assuming a proton size which increases with increasing density. We have identified the origin of the variable proton size through the structure function obtained from dynamical six-quark N - N studies in the spirit of the independent pair approximation. We could probably improve our results if we recalculate meson effects using the quark structure functions given (say) by the six-quark IPA model. This item is a topic for further investigation.

In addition, one could study the predictions of models based on quark substructure for quasielastic scattering. In the quasifree regime, nuclear models produce a good description of the data as long as realistic nucleon interactions, including charge exchange, are incorporated in the final-state interaction [16]. Unlike the charge form factor, two-body charge operators are expected to play a much smaller role here, principally because this is the dominant channel and there is little interference. The combination of the two regimes provides a critical test for models of structure and dynamics in light nuclei.

ACKNOWLEDGMENTS

We wish to thank C. Horowitz and others for valuable discussions. This work is supported in part by the U.S. Department of Energy and by the National Science Foundation.

- [1] J.S. McCarthy, I. Sick, and R.R. Whitney, *Phys. Rev. C* **15**, 1396 (1977).
- [2] I. Sick, in *Few Body Systems and Nuclear Forces II*, Lecture Notes in Physics Vol. 87, edited by H. Zingl, M. Haftel, and H. Zankel (Springer, Berlin, 1978), p. 236.
- [3] J.L. Friar, B.F. Gibson, E.L. Tomusiak, and G.L. Payne, *Phys. Rev. C* **24**, 665 (1981).
- [4] R.B. Wiringa, *Phys. Rev. C* **43**, 1585 (1991).
- [5] J. Carlson, *Nucl. Phys.* **A522**, 185c (1991).
- [6] R. Schiavilla and D.O. Riska, *Phys. Lett. B* **244**, 373 (1990).
- [7] L.S. Kisslinger, W.-H. Ma, and P. Hoodbhoy, *Nucl. Phys.* **A459**, 645 (1986); W.-H. Ma and L. S. Kisslinger, *ibid.* **A531**, 493 (1991); W.-H. Ma, Q. Wu, and L.S. Kisslinger, *ibid.* **A560**, 997 (1993).
- [8] H. Pirner and J.P. Vary, *Phys. Rev. Lett.* **46**, 1376 (1981).
- [9] W. Koepf, L. Wilets, S. Pepin, and Fl. Stancu, *Phys. Rev. C* **50**, 614 (1994).
- [10] W. Koepf and L. Wilets, *Phys. Rev. C* **51**, 3445 (1995).
- [11] S. Pepin, Fl. Stancu, W. Koepf, and L. Wilets, *Phys. Rev. C* **53**, 1368 (1996).
- [12] L. Wilets, *Nontopological Solitons* (World Scientific, Singapore, 1989).
- [13] R. Blankenbecler and S. Brodsky, *Phys. Rev. D* **10**, 2973 (1974); G. Farrar and D. Jackson, *Phys. Rev. Lett.* **35**, 1416 (1975); A. Vainstein and V. Zakharov, *Phys. Lett.* **72B**, 368 (1978).
- [14] I.E. Lagaris and V.R. Pandharipande, *Nucl. Phys.* **A351**, 331 (1981).
- [15] J. Carlson, *Phys. Rev. C* **38**, 1879 (1988).
- [16] J. Carlson and R. Schiavilla, *Phys. Rev. Lett.* **68**, 3682 (1992); *Phys. Rev. C* **49**, R2880 (1994).